

A PV Temperature Prediction Model for BIPV Configurations, Comparison with Other Models and Experimental results

S. Kaplanis^a, E. Kaplani^b

^aRenewable Energy Systems Laboratory, TEI of Western Greece,
Patra, Greece

^bEngineering Division, School of Mathematics, University of East Anglia,
Norwich, UK

Abstract

The temperatures of c-Si and pc-Si BIPV configurations of different manufacturers were studied when operating under various environmental conditions. The BIPV configurations formed part of the roof in a Zero Energy Building, (ZEB), hanged over windows with varying inclination on a seasonal basis and finally two identical 0.5kW_p PV generators were mounted on a terrace in two modes: fixed inclination and sun-tracking. The PV and ambient temperatures, T_{pv} and T_a , respectively, the intensity of the global solar radiation on the modules, I_T , and the wind velocity on their surface, v_w , were monitored for 2 years. The effect of the intensity, I_T , the PV module inclination and v_w on T_{pv} was investigated. The values of the coefficient f relating T_{pv} and I_T , were determined and argued for the configurations studied. A theoretical model was elaborated to predict T_{pv} and f for the cases of PV modules embedded on a roof, hanging over the windows and in free standing configurations. The effect of v_w on f dominated for PV modules mounted on the terrace compared to the BIPV configurations in wind protected areas.

Keywords: PV temperature prediction, PV inclination, BIPV, wind effect, PV roofs

INTRODUCTION

The issue of PV module temperatures, T_{pv} , developed when operating under field conditions was investigated in a number of projects where different formulas for its determination were provided [1-8]. The T_{pv} profiles were well understood by building the Energy Balance Equation for transient and steady state conditions taking into account the power and heat generated in a PV module operating under global solar radiation intensity on it, I_T , in ambient temperature, T_a , and wind speed, v_w [9-11]. Figs.1(a),(b),(c) show the various BIPV configurations monitored and studied in this project. In other ZEB configurations, the PV modules are either embedded in facades being part of the building structure through sophisticated designs operating as PV/T power and heat co-generation systems [11] or the PV modules are placed at a small distance about 10-15 cm from the roof tiles. Published works deal with the T_{pv} functional dependence on I_T and v_w in various environments like in [5-8,11,12]. Especially, v_w strongly affects the heat convection coefficients, $h_{c,f}$ and $h_{c,b}$ in the front and back side of the module and therefore T_{pv} . However, the equations proposed take the v_w effect on $h_{c,f}$ and $h_{c,b}$ to be in a linear form, while other parameters, too, are very important for consideration such as the geometry of the module, the air flow details as for example air free flow, forced flow, laminar and turbulent modes, the wind direction with respect to the PV module and also the inclination of the module with respect to horizontal, as was investigated in [13]. In some works, the type of PV cell, Si or CdTe was specified in the formulas proposed for the T_{pv} prediction along with the BIPV configuration

which resulted in slight modifications [5,6]. It is underlined that the wind speed, v_w , and the solar irradiance on the modules, I_T , have a 2nd order effect on T_{pv} through their effect to η_{pv} . The T_{pv} as a notion has to be clarified as the temperature in the front, the back side of the module and the semiconductor temperature differ. Thus, there is a need for more systematic and comparative analysis as it regards the effect of the environmental conditions in the BIPV performance where the explicit and implicit inter-relationships between, T_{pv} , I_T , v_w and the PV module inclination should be included. An approach to estimate T_{pv} for PV systems in facades was presented in, [14], using the relationship given in [5]. A wider analytic approach for the f factor and T_{pv} prediction is presented in this paper for various BIPV configurations using:

1. a set of co-related equations which fully describe the heat propagation from the PV inner core to the environment, and
2. a relationship, taking as a reference the ambient temperature, T_a , and an elaborated mathematical expression for the factor $f=f(v_w, T_{pv}, I_T, \eta_{pv})$, as discussed below,

$$T_{PV} = T_a + f \cdot I_T \quad (1)$$

f may not be given by a closed mathematical formula due to its implicit dependence on the above quantities. Instead, an empirical function of f applicable to any conditions was determined in this paper through regression analysis of measured values, T_{pv} , I_T , v_w , T_a . In

another approach a theoretical model might be developed with a set of equations to be used for the determination of the f and T_{pv} by means of a complete set of heat transfer and IR radiation expressions associated to the PV module energy balance equation, as analytically elaborated in [13] taking into account all possible environmental condition and geometries. In this research project the values that f takes up in various types of BIPV installations were determined experimentally analyzing systematically a time series of I_T , T_a , T_{pv} and v_w data on the basis of eq.(1), for

$f=f(v_w, T_{pv}, I_T, \eta_{pv})$. An algorithmic approach to predict T_{pv} is outlined in the next Section using expressions through which f may be estimated as an implicit function of the environmental conditions. Conclusively, T_{pv} experiences explicit and implicit dependence on the environmental conditions. Its impact to PV power performance may be estimated through eq.(1) from the f values theoretically produced or experimentally developed as functions of v_w , η_{pv} and T_{pv} , in a second order effect [4,5,11,15].

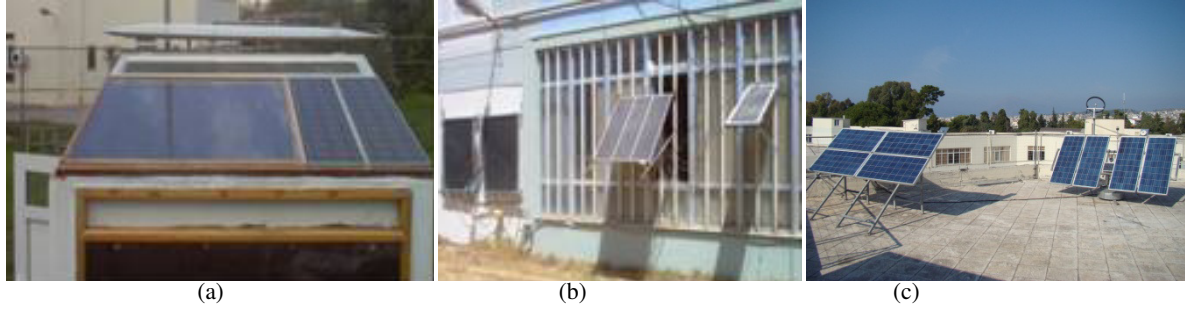


Fig. 1(a) BIPV embedded in a roof, (b) BIPV as shadow hangers, (c) BIPV fixed and sun-tracking on a terrace

THE THEORETICAL MODEL TO PREDICT f and T_{pv} in BIPV CONFIGURATIONS

It is important to provide good estimates of the power performance of PV modules integrated into ZEB structures taking into account I_T , T_{pv} , v_w , T_a and where appropriate the inclination of the PV modules. The PV modules, as shown in Figs.1(a),(b) have their back side fully or partially wind protected. An insulated back cover below the PV plane stands for the ceiling, Figs.2(a),(b). Heat is extracted via air free flow in laminar mode through an orifice pattern. The warm air is self-pumped through the orifice and is self-circulated by free convection within the room for space heating or in warm days it is self-pumped out of the building through the solar chimney, Fig.1(a), [11]. The room temperature inside the building plays the role of T_a in eq.(1). The front side of the PV modules faces the free environment and heat may be extracted by air free flow or air forced flow either under laminar or turbulent mode to be determined from the environmental conditions prevailing each time. The front PV side may experience higher heat rate extraction than its back side which forms part of the internal building structure. The natural ventilation inside the ZEB test cell reduces the T_{pv} rise at the PV back side and hence limits the drop in η_{pv} , thus attaining a partial recuperation. This solar roof design is advantageous over the design where the PV modules are mounted upon the roof with an air gap of about 10-15cm from the tiles, as it operates as a PV/T. In both cases, the PV back side is wind protected contrary to the front one. For the BIPV configuration where the PV modules are deployed over windows,

their inclination, β , with respect to the horizontal, Fig.1(b), changes seasonally so that the direct solar radiation to be normal on the PV plane, satisfying the condition, $\beta=\varphi-\delta$, where φ is the latitude of the site and δ is the sun's declination angle, easily calculated.

The heat convection coefficients $h_{c,f}$ and $h_{c,b}$ for the inclined front and back sides, should be determined by proper expressions as those in sub-sections 2.1.1 and 2.1.2 in [13] which cover the entire range of Ra values, including the transition from laminar to turbulent flow through the estimation of the critical Grashof number Gr_c included in the Nu expression, [16,17]. The inclination effect enters through the determination of the Nu number at air flow modes from both the front and back PV sides. The 3rd and 4th BIPV examined have the form of small PV generators 0.5 kW_p, aesthetically mounted on a terrace as fixed and sun-tracking. The estimation of the $h_{c,f}$, $h_{c,b}$ and $h_{r,f}$, $h_{r,b}$ coefficients, dependent on T_{pv} , v_w , inclination and orientation of the modules follows the analysis in [13].

An outline of the proposed model to predict T_{pv} based on the determination of the f coefficient

The energy balance equation for steady state conditions, shown in eq.(4), takes into account the solar radiation on the PV module, the power produced, the heat losses due to conduction, convection, and the net IR radiation exchange with the environment. U_f and U_b below stand for the sum of heat and radiative loss coefficients for the front and back sides, respectively, where:

$$U_f = h_{c,f} + h_{r,f} \quad \text{and} \quad U_b = h_{c,b} + h_{r,b} \quad (3)$$

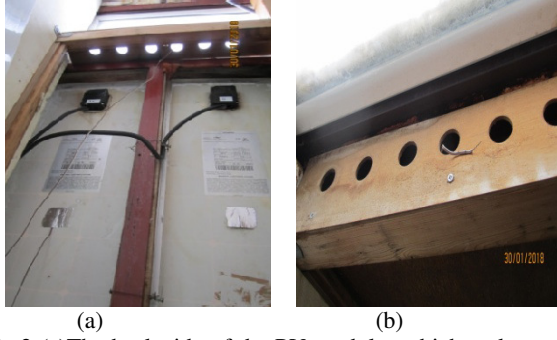


Fig.2 (a)The back side of the PV modules which make part of the roof in a ZEB cell. (b) The wooden case forms the ceiling. The higher end of the case ends to a number of air orifice for the heated by the module air to expand.

A theoretical model is developed based on eqs.(4)-(9) to predict effectively T_{pv} and determine f for any PV configuration at steady state conditions.

$$I_T = \eta_{pv} I_T + U_f(T_f - T_a) + U_b(T_b - T_a) \quad (4)$$

$$\text{For } T_f = T_b + \delta T \quad (5)$$

$$T_b = T_a + \frac{(1-\eta_{pv})I_T}{U_f+U_b} - \frac{U_f}{U_f+U_b} \delta T \quad (6)$$

T_b is chosen instead of T_f as it was measured and recorded by the monitoring system during this project.

A considerable effort has been made to develop easily handled expressions to determine T_{pv} by means of the f coefficient. The combination of eqs.(1) and (6) gives that f may be expressed by:

$$f = \frac{1-\eta_{pv}}{U_f+U_b} - \frac{U_f}{(U_f+U_b)I_T} \delta T \quad (7)$$

The first term above is considered as the first approach value of f , f_o , where,

$$f_o = \frac{1-\eta_{pv}}{U_f+U_b} \quad (8)$$

$$f = f_o - \left[\frac{U_f}{(U_f+U_b)I_T} \right] \delta T \quad (9)$$

For low wind speeds U_f and U_b take values around $10\text{W/m}^2\text{K}$, while the temperature difference in the front and back side, δT , experimentally measured was around $\pm 2\text{-}3^\circ\text{C}$. The sign changes due to wind velocity direction either forward or leeward. Therefore, for I_T in the range of $800\text{-}10^3\text{W/m}^2$ and $\eta_{pv} = 0.15$, f falls as easily calculated in the range of $[0.040, 0.044] \text{m}^2\text{K/W}$ which is the region of f values experimentally

determined in BIPV cases, such as those in Figs.1(a),(b). For v_w of about 2.5m/s , U_f and U_b values increase and f reduces to values of about $0.028\text{m}^2\text{K/W}$ and for $v_w > 5\text{m/s}$ to values in the range of $0.015\text{-}0.020 \text{m}^2\text{K/W}$, as this is the case of PV systems in Fig.1(c).

The f factor was investigated as a product of 2 functions shown in eq.(10) and validated comparing its values with experimentally produced ones and also with those from other 2 well known model functions [4,5].

$$f = \frac{1-\eta_{pv}}{U_f+U_b} - \left[\frac{U_f}{(U_f+U_b)I_T} \right] \delta T = f(v_w) f(\eta_{pv}, T_{pv}, I_T, v_w) \quad (10)$$

The first one is a function of v_w , and the second of η_{pv} implicitly dependent on T_{pv} , and in second order on I_T and v_w . Expanding f in Taylor series around the point $v=v_w$ and estimating the first derivative for the average values of the recorded environmental data ($T_a = 20^\circ\text{C}$ and $I_T = 800\text{W/m}^2$) at that point, the following expression is obtained.

$$f = f(v_w) + \left(\frac{df}{d\eta_{pv}} \right)_m \delta \eta_{pv} = f(v_w) - \delta \eta_{pv} / (U_f + U_b) = f(v_w) (1 - \delta \eta_{pv} / (1 - \eta_{pv,m})) \quad (11)$$

The $f(v_w)$ value obtained from the rational expression, eq.(12) whose coefficients were obtained by regression analysis of the 2 years recorded data T_b , v_w , I_T , T_a , corresponds to the average values of T_a and I_T .

$$f(v_w) = \frac{a+bv_w}{1+cv_w+dv_w^2} \quad (12)$$

where, $a = 0.0375$, $b = 0.0081$, $c = 0.2653$, $d = 0.0492$.

Finally, the f coefficient is estimated by:

$$f = f(v_w) \left(1 - \frac{d\eta_{pv} \delta T_{pv}}{1 - \eta_{pv,m}} \right) \quad (13)$$

δT_{pv} may be expressed through the differences between the environmental conditions during the experiment and the average environmental conditions, as said above.

The above formula may be used for the prediction of T_{pv} and especially in this case T_b for any environmental conditions, I_T , T_a , v_w . Eq.(11) is also used for PV modules other than c-Si or pc-Si with different η_{pv} as it modifies the constants in the rational expression for f .

EXPERIMENTAL RESULTS - DISCUSSION

1. BIPV configuration with the PV modules making part of the roof, Fig.1(a).

f for clear sky, almost clear sky or partly cloudy conditions during the 2 years data monitoring even with v_w up to 5m/s for any day of the year takes values in the domain $0.0420 \pm 0.006 \text{ m}^2\text{K/W}$ which differ considerably from the cases of PV mounted on terrace as to be shown below.

Such values are also valid for PV modules serving as shadow hangers over windows with very low angle of inclination, e.g. 0° - 15° , in wind protected areas at low wind speeds $<1.0 \text{ m/s}$, as given in Table 1 and in Fig.5 for several inclination angles.

2. For PV configurations with the modules in the free environment, and not in wind protected areas, f may be obtained from eqs.(11)-(13), taking into account the operating conditions each time.

The proposed expressions of eqs.(11)-(13) hold for any BIPV with PV modules mounted on fixed or sun-tracking frames or in solar roofs. Based on the above, for the BIPV of Fig.1(a), for $I_T = 800\text{W/m}^2$ on a PV roof with $\eta_{pv} = 0.15$, the uncertainty in the estimation of T_{pv} equals to $\Delta T_{pv} = \pm 0.006 \times 800 = \pm 4.8^\circ\text{C}$. For, $\delta\eta_{pv}/\eta_{pv} = -0.4\%$ ΔT_{pv} it becomes $\delta\eta_{pv} = \eta_{pv} \times 1.92\% = 0.15 \times 0.0192 = \pm 0.3\%$ which in fact is a relatively narrow domain in which η_{pv} values were estimated.

Figs.3(a)-(d) show the T_{pv} vs I_T for an embedded PV roof for several days within a year. The slope, f , lies in the range theoretically predicted above. Fig.3(c) shows slight deviations from the linearity due to changes in the sky conditions and the environment. Such cases were also observed in [18,20]. However, the general linear form still holds and the slope is kept within the interval of values specified above. In general, the abscissa is equal to T_a , at the time the PV starts running, while the slope i.e. the rate T_{pv} changes is higher in cold environment rather than warm, in agreement to the theoretical model outlined. f decreases with increasing v_w according to eq.(12) for PV modules either in a free environment or for PV integrated into a façade or roof.

Figs.4(a),(b),(c) show $(T_{pv}-T_a)$ vs I_T , v_w vs hour and the f vs the hour of the day for free standing pc-Si PV modules fixed and sun-tracking on a terrace for July. In both PV systems, f experiences considerable changes, mainly due to the v_w . The f values in the fixed and sun-tracking systems at the same hour differ due to the different wind speed direction with reference to the PV plane.

$(T_{pv}-T_a)$ vs I_T for free standing PV for the representative day of July shows sub-linear behaviour and this is due to the higher v_w values around 3-4m/s for the period after 10am when I_T takes values higher than 500 W/m^2 for the fixed system and 850W/m^2 for the sun-tracking. The wind effect decreased the slope of the T_{pv} vs I_T curve. The f values are about $0.035\text{Km}^2/\text{W}$ for the fixed system and $0.030 \text{ Km}^2/\text{W}$ for the sun-tracking at 10am when v_w is 2.5m/s . During that period the angle of wind direction with respect the sun-tracker is 30 - 60° on the

back side, where T_{pv} is measured, while for the fixed system the wind strikes the front surface in around 80 - 90° , which implies lower rate to heat extraction [13]. For higher v_w in the range of 2.5 - 4m/s the f coefficient takes values of about 0.022 - $0.025 \text{ Km}^2/\text{W}$ very close for both configurations as the front side is the windward side for both. When v_w is low, see Figs.4(b) morning hours, the f value for the fixed system is higher due to the dependence of the Ra number on the inclination which in this case is lower for the fixed system, 38° compared to the sun-tracking system inclination around 50 - 60° for the morning hours. The difference in f for both systems vanishes as $v_w > 2.5\text{m/s}$.

On the other hand, $(T_{pv}-T_a)$ vs I_T may change to super-linear when low v_w values prevail during noon compared to the morning and afternoon v_w values. That was verified with the experimental data analyzed.

BIPV configurations with PV modules mounted in wind protected zones or hanging over windows for shadowing and power production were monitored. The data analysis of T_{pv} vs I_T for cases $v_w < 1\text{m/s}$ gave the results for f coefficient shown in Table 1. Fig.5 shows $(T_{pv}-T_a)$ vs I_T for various inclinations. The f coefficient decreases as β increases from 0° as argued before. It is very interesting to realize that for β around 45° f takes its lowest value due to the fact that the air flow past the PV module back side reaches the stage to turn into turbulent, while its highest value is for small nearly horizontal inclinations. For inclination higher than 45° f increases slowly.

Table 1. Values of the f coefficient for PV modules as shadow hangers in wind protected areas for various inclinations

β	$f \pm \sigma_f$
0°	0.044 ± 0.004
16°	0.040 ± 0.002
26°	0.033 ± 0.003
36°	0.025 ± 0.002
47°	0.023 ± 0.002
$>70^\circ$	0.034 ± 0.005

The results of T_{pv} prediction given by the proposed model through the determination of the f coefficient were compared for validation with measured values during the representative days of the months of the year and also with the T_{pv} provided by the models [5,6]. The results for July for both BIPV configurations are given in Table 2 where it is obvious that the proposed model has an overall very good prediction performance compared to the other models.

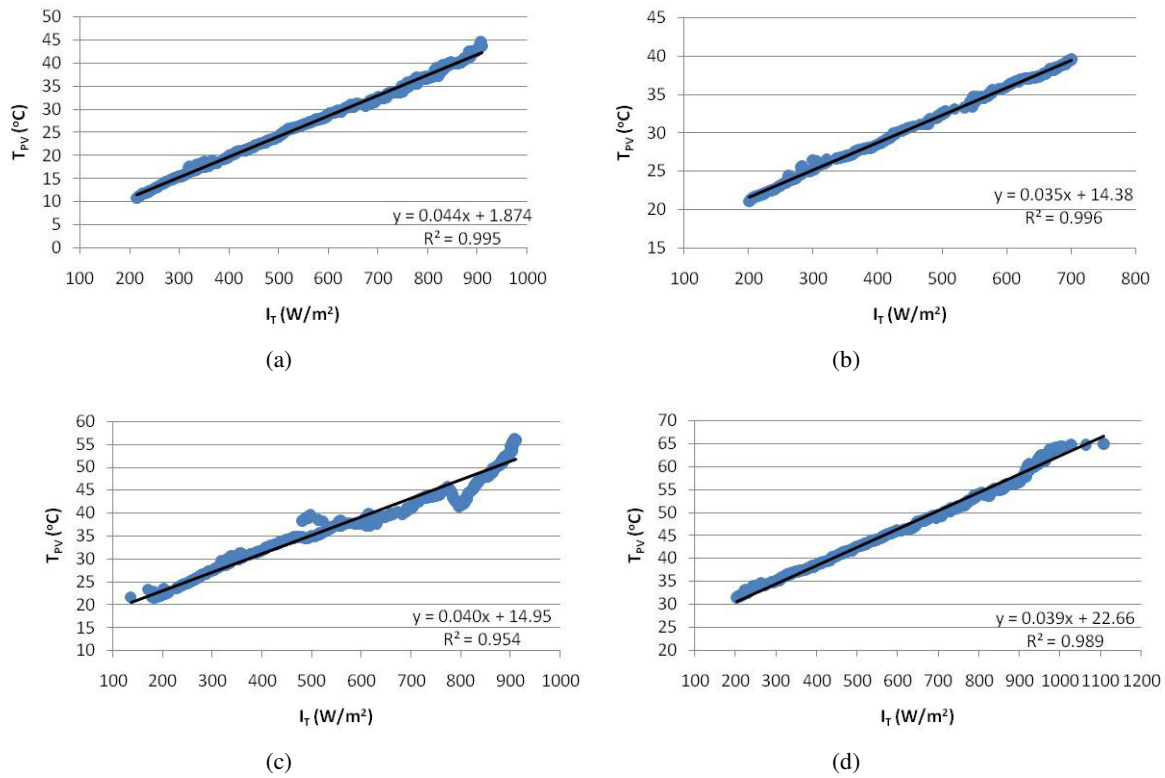


Fig.3 T_{pv} vs I_T in an embedded PV roof for the (a) 18-3-17, (b) 17-5-16, (c) 4-10-16, (d) 9-7-16

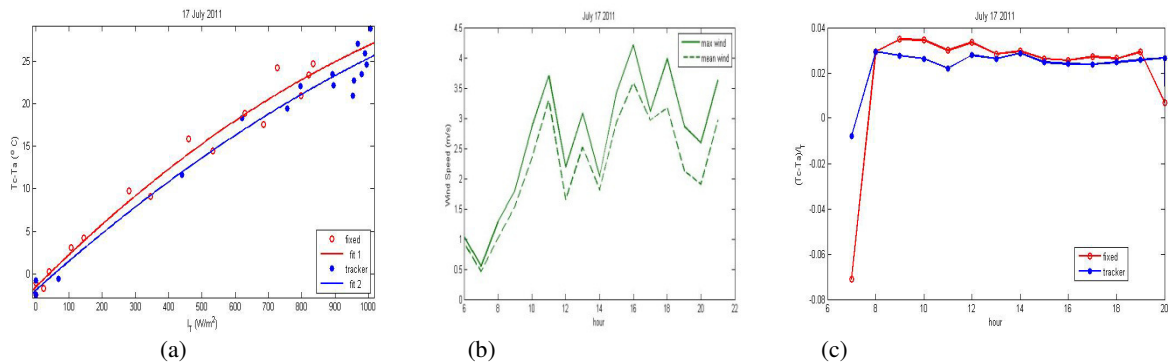


Fig.4 (a) $T_c - T_a$ vs I_T for the month July for pc-Si PV modules on the terrace. For both fixed and sun-tracking frames the function is sub-linear due to the high v_w after 10am when I_T takes values above 400W/m^2 . (b) provides the v_w vs hour of the day and (c) shows the changes in f from 0.038 morning hours when v_w is low to 0.022 for the rest of the day when $v_w > 2.5\text{m/s}$. The lines correspond to fixed and sun-tracking frames.

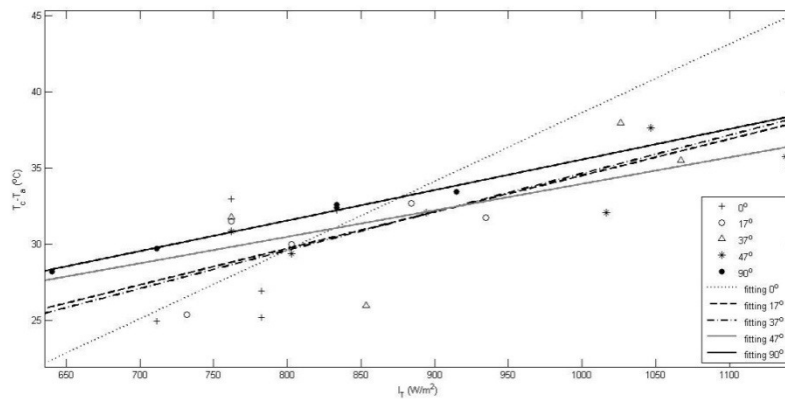


Fig.5 $(T_{PV} - T_a)$ vs I_T for different PV inclination angles, for c-Si PV modules operating in free space -wind protected.

Table 2. Comparison of predicted T_{pv} values by this model, and those in [5,6] with measured ones in July from a fixed and a sun-tracking PV system on a terrace.

Time hour	Model [6] T_{pv} (°C)		Model [5] T_{pv} (°C)		Measured T_{pv} (°C)		Proposed Model T_{pv} (°C)	
	Fixed	Tracking	Fixed	Tracking	Fixed	Tracking	Fixed	Tracking
10	10.1	19.8	12.1	23.7	14.0	22.5	13.0	26.2
12	17.3	23.3	19.9	26.8	23.0	27.0	21.5	28.1
14	22.2	27.0	21.0	25.3	24.0	29.0	24.9	31.0
16	15.2	21.5	16.0	21.5	17.0	23.0	19.0	26.8

CONCLUSIONS

The paper outlines a theoretical model developed for the PV module temperature, T_{pv} , prediction taking into account the environmental conditions, i.e. ambient temperature, T_a , solar irradiance on the module, I_T , and wind speed, v_w , on the PV module and their effect to the PV efficiency. A set of equations fully simulate the heat propagation from the PV module to the environment and through iterations give the front, back side and Si temperatures. To predict T_{pv} a regression analysis of recorded data of c-Si and pc-Si modules gave a formula to determine the correlation factor between T_{pv} and I_T . The formula is split in 2 functions, the first with argument the wind speed in a rational function and the second the efficiency change due to the effect of the environmental factors. The values of this factor differ according to the BIPV configuration. BIPV serving as roofs and PV generators gave high f values in the range $0.040 \pm 0.006 \text{ m}^2\text{K/W}$. Same values were obtained experimentally and theoretically for BIPV systems acting also as shadow hangers over windows placed in wind protected zones with small inclination $<16^\circ$. For small BIPV systems of 0.5 kW_p placed on the terrace either in fixed position or on sun-tracking frames the predicted T_{pv} values through the determination of f were compared with other 2 known models and the experimental results and showed very good prediction for both BIPV modes. The formula for f is applicable to other types of PV cells. The f coefficient ranges from almost $0.01 \text{ m}^2\text{C/W}$ for free standing PV arrays at strong wind speeds, $v_w > 7 \text{ m/s}$, up to around $0.05 \text{ m}^2\text{C/W}$ for the case of flexible PV modules which make part of the roof in a BIPV system. In addition, f depends implicitly on I_T , the inclination angle, β , the type of heat convection; that is, natural or forced flow, the pattern of air flow past the PV panel, i.e. laminar or turbulent, the relative wind direction with respect to the PV module surface and the type of the BIPV configuration. The effect in f is bigger for free standing systems rather than for wind protected systems where only the front side is directly subjected to the wind.

REFERENCES

- [1] K. Emery et al.: Temperature dependence of photovoltaic cells, modules and systems. Photovoltaic Specialists Conference, 1996, Conference Record of the 25th IEEE.
- [2] A. R. Wilshaw, J. R. Bates, and N. M. Pearsall: Photovoltaic module operating temperature effects. Proceedings of the Eurosun '96, pp. 940–944, Munich, Germany, 1996.
- [3] E.E. van Dyk, E.L. Meyer: Long-term monitoring in Photovoltaic modules in South Africa. S.Afr.J.Sci. 96, 198-200,2000.
- [4] A.R. Gxasheka, E.E. van Dyk, E.L. Meyer: Evaluation of performance parameters of PV modules deployed outdoors. Renewable Energy 30, 2005, pp.611-620
- [5] D.L.King et al.: Photovoltaic Array Performance Model. SAND2004-3535.
- [6] D. Faiman: Assessing the outdoor operating temperature of photovoltaic modules. Progress in Photovoltaics: Research and Applications, Vol. 16, no. 4, pp. 307–315, 2008.
- [7] E. Skoplaki and J. A. Palyvos: On the temperature dependence of photovoltaic module electrical performance: a review of efficiency/power correlations. Solar Energy, vol. 83, no. 5, pp. 614–624, 2009.
- [8] M. Mattei, G. Notton, C. Cristofari, M. Muselli, and P. Poggi: Calculation of the polycrystalline PV module temperature using a simple method of energy balance. Renewable Energy, vol. 31, no. 4, pp. 553–567, 2006.
- [9] S. Kaplanis: Determination of the electrical characteristics and thermal behaviour of a c-Si cell under transient conditions for various concentration ratios. Int. J. Sustainable Energy, 35, 2016, pp.887-992.
- [10] G. Tina: A Coupled Electrical and Thermal Model for Photovoltaic Modules. J. of Sol. Energy Engineering 132(2):024501, 2010.
- [11] S. Kaplanis, E. Kaplani (eds): Renewable Energy Systems: Theory, Innovations and Intelligent Applications. NOVA Science Publishers, N.Y., 2013
- [12] G. Ciulla, V. Lo Brano, and E. Moreci: Forecasting the cell temperature of PV modules with an adaptive system. International Journal of Photoenergy, Vol. 2013, Article ID 192854, 10 pages, 2013
- [13] E. Kaplani, S. Kaplanis: Thermal modelling and experimental assessment of the dependence of PV module temperature on wind velocity and direction, module orientation and inclination. Solar Energy 107, 443-460.
- [14] V. Benda: Proc. Inno Week 2013, Patra, Greece, ISSN:978-969-7801-24-1
- [15] E. Radziemska: The effect of temperature on the power drop in crystalline silicon solar cells. Renewable Energy, 28, 2003, pp 1-12.
- [16] A.A. Kendouch: Theoretical Analysis of heat and mass transfer to fluids flowing across a flat surface. Int.l J. of Thermal Sciences, 48, 2009, 188-194.

- [17] E. Sartori: Convection coefficient equations for forced air flow over flat surfaces. *Sol. Energy* 80, 1063-1071.
- [18] S.Armstrong, W.G.Hurley: A thermal model for photovoltaic panels under varying atmospheric conditions. *Applied Thermal Engineering*, 30, 2010, 1488-1495.
- [19] J. Kaldellis, M. Kapsali, K. Kavadias: Temperature and wind speed impact on the efficiency of PV installations. Experience obtained from outdoor measurements in Greece. *Renewable Energy*, 66, 2014, 612-624.
- [20] C. Schwingshackl et al.: Wind effect on PV module temperature: Analysis of different techniques for an accurate estimation. *Energy Procedia* 40, 2013, 77-86.

Addresses of the authors

S. Kaplanis, Renewable Energy Systems Laboratory, TEI of Western Greece, Meg. Alexandrou 1, Patra, Greece, kaplanis@teiwest.gr

E. Kaplani, Engineering Division, School of Mathematics, University of East Anglia, Norwich, NR4 7TJ, UK e.kaplani@uea.ac.uk